A Generalized Treatment of Magneto-Optical Transmission Filters

Matthew D. Rotondaro,* Boris V. Zhdanov, and Randall J. Knize

US Air Force Academy, Laser and Optics Research Center, 2354 Fairchild Dr., Ste. 2A31, USAF Academy, Colorado 80840, USA
*matthew.rotondaro@usafa.edu

This work has constructed a model for the theoretical analysis of generalized magneto-optical transmission (GMOT) filters for any relative angle between the light beam and the applied magnetic field. This model was experimentally validated and shows good agreement between the theoretical predictions and the experimental spectra. In addition, the value of examining magneto-optical filters for arbitrary angle cases was demonstrated by revealing an optimized filter with an equivalent noise bandwidth of 0.56 GHz which is approximately a factor of two better than those previously reported.

1. BACKGROUND

Magneto-optical scattering has been extensively studied with the dominant emphasis on the Faraday Effect in atomic media. The Faraday Effect occurs when a resonant light beam is propagated through an atomic medium parallel to an applied magnetic field. These studies, in addition to basic theory [1-4], have examined a wide area of applications such as atmospheric LIDAR [5-7], communications [8], quantum optics [9], helioseismology [10], etc. While the Faraday Effect has dominated the study there has also been some examination of the Voigt Effect which occurs when a resonant light beam is propagated through an atomic medium perpendicular to the applied magnetic field. An analysis of the Voigt Effect was conducted by Yamamoto [11], its usefulness as a filter for 455 nm cesium was examined by Menders [12] and the detection of atomic species by Kankar[13]. The final and most general case where the resonant light beam is propagated though the atomic medium at an angle θ relative to the applied magnetic field where $0 < \theta < 90$ degrees. The only examination of a fully generalized solution was presented by Palik [1]. Palik provides a framework for the solution for arbitrary angle but does not provide a complete solution or theoretical results. This work extends the magneto-optical filter work for arbitrary angle of incidence relative to the applied magnetic field and offers experimental results to validate the calculations.

2. THEORY

A complete analysis of magneto-optical filters can be broken into two distinct parts. The first part is the characterization of the dispersive medium and the second is the propagation of a plane wave through the dispersive medium. The first part, the characterization of the dispersive medium has been demonstrated throughout the literature. These characterizations vary from very simple two level analyses to robust calculations which take into account atomic hyperfine splitting, Zeeman splitting, moving particles (Doppler Effect), the Boltzmann distribution of the energy level population and the inclusion of the line strength for each dipole allowed transition. The second part, the propagation of a plane wave through a dispersive medium, is always evaluated in one of two limiting cases, Faraday or Voigt. The feature that distinguishes these two cases for Faraday the plane wave propagates parallel to the applied magnetic field and for Voigt the plane wave propagates perpendicular to the magnetic field. This work will break with previous work and demonstrate a theoretical treatment for cases when the angle between the direction the plane wave propagates and the magnetic field is between 0 and 90 degrees.

A. Plane Wave Propagation

This derivation follows the work by Palik [1]. Palik derives a case where the magnetic field is fixed and the plane wave direction of propagation is arbitrary. This work will modify the derivation so that the result has a fixed plane wave direction of propagation and the magnetic field is rotated. This change produces a framework which is much more amenable to laboratory work. The development begins with Maxwell's equations.

$$\nabla \times \boldsymbol{E} = -\mu_0 \frac{\partial \boldsymbol{H}}{\partial t}, \qquad \nabla \times \boldsymbol{H} = \epsilon \frac{\partial \boldsymbol{E}}{\partial t} + \boldsymbol{J}$$
$$\nabla \cdot \boldsymbol{E} = \frac{\rho}{\epsilon}, \qquad \nabla \cdot \boldsymbol{B} = 0 \tag{1}$$

The case we are interested in examining is an atomic vapor with no current or charge density with a monochromatic plane-wave solutions given by $e^{i(\boldsymbol{k}\cdot\boldsymbol{r}-\omega t)}$. Substituting this plane wave solution into Maxwell's equations results in the wave equation,

$$\boldsymbol{k} \times (\boldsymbol{k} \times \boldsymbol{E}) + \frac{1}{\epsilon_0}\left(\frac{\omega}{c}\right)^2 \epsilon \cdot \boldsymbol{E} = 0. \tag{2}$$

From here, we assume a light beam that lies in the xz-plane making an angle with the z-axis, a magnetic field parallel to the z-axis and define the complex index of refraction n given by

$$n^2 = \left(\frac{c}{\omega}\right)^2 \left(k_x^2 + k_y^2 + k_z^2\right). \tag{3}$$

Also, with the magnetic field aligned along the z-axis the dielectric tensor can be cast in the gyrotropic form [1]

$$\epsilon = \begin{bmatrix} \epsilon_x & \epsilon_{xy} & 0 \\ -\epsilon_{xy} & \epsilon_x & 0 \\ 0 & 0 & \epsilon_z \end{bmatrix} \tag{4}$$

This allows the dispersion equation to be cast in matrix form

$$\begin{bmatrix} \frac{\epsilon_x}{\epsilon_0} - n^2\cos^2\theta & \frac{\epsilon_{xy}}{\epsilon_0} & n^2\sin\theta\cos\theta \\ -\frac{\epsilon_{xy}}{\epsilon_0} & \frac{\epsilon_x}{\epsilon_0} - n^2 & 0 \\ n^2\sin\theta\cos\theta & 0 & \frac{\epsilon_z}{\epsilon_0} - n^2\sin^2\theta \end{bmatrix} \begin{bmatrix} E_x \\ E_y \\ E_z \end{bmatrix} = 0. \tag{5}$$

This matrix represents a plane wave which propagates at an angle θ relative to the applied magnetic field along the z-axis. This formalism is not the optimum choice when an experimental setup is considered. In a laboratory environment, a laser beam is passed through a polarizer, vapor cell and then through another polarizer. Polarizers are two dimensional in nature but this treatment, in general, requires a three dimensional polarization of the incident electric field. This contradiction is solved by starting with the polarization aligned along the x and y-axis (two dimensions) then rotating the x-axis component to produce a polarization component that lies along the z-axis. This transformation results in a fixed beam that propagates along the z-axis with polarization along the x and y-axis and the magnetic field is rotated through the xz-plane.

To begin this transformation, we define the z-axis as the direction the plane wave propagates and the x and y-axis as the direction of the electric field's polarization. Once this choice is made it is a simple matter to transform the plane wave using a transformation matrix that rotates the laser beam around the y-axis.

$$\begin{bmatrix} \cos\theta & 0 & \sin\theta \\ 0 & 1 & 0 \\ -\sin\theta & 0 & \cos\theta \end{bmatrix} \qquad (6)$$

Ultimately, this transformation also maps the dispersion matrix from a magnetic field reference frame to the plane wave's reference frame. The laser plane wave $\mathbf{E_0} = (E_x, E_y, 0)$ is fixed and the magnetic field rotates around the y-axis and the B field lies in the xz-plane. Note, E_x and E_y are complex quantities. Therefore, this formalism will apply to right and left handed circularly polarized light as well as linearly polarized light. Applying the transformation to the wave equation results in

$$\begin{bmatrix} \left(\frac{\epsilon_x}{\epsilon_0} - n^2\right)\cos\theta & \frac{\epsilon_{xy}}{\epsilon_0} & \frac{\epsilon_x}{\epsilon_0}\sin\theta \\ -\frac{\epsilon_{xy}}{\epsilon_0}\cos\theta & \frac{\epsilon_x}{\epsilon_0} - n^2 & -\frac{\epsilon_{xy}}{\epsilon_0}\sin\theta \\ \left(n^2 - \frac{\epsilon_z}{\epsilon_0}\right)\sin\theta & 0 & \frac{\epsilon_z}{\epsilon_0}\cos\theta \end{bmatrix}\begin{bmatrix} E_x \\ E_y \\ 0 \end{bmatrix} = 0. \qquad (7)$$

The solution to this set or equations is found by setting the determinant of the matrix to zero and solving for the two roots of n^2. Once the roots n_1^2 and n_2^2 are found, each root is successively substituted back into the matrix and the Eigenvector corresponding to the zero eigenvalue is evaluated. In general the Eigenvectors are dependent on θ and will be designated $\mathbf{Ev_1}$ and $\mathbf{Ev_2}$.

After the Eigenvectors are known, the resulting electric field $\mathbf{E_f}$ can be constructed by projecting the initial electric field $\mathbf{E_0}$ onto the Eigenvectors and propagating the field along the z axis.

$$\mathbf{E_f}(z,\theta) = \mathbf{Ev_1}\frac{\mathbf{E_0}\cdot\mathbf{Ev_1^*}}{\mathbf{Ev_1}\cdot\mathbf{Ev_1^*}}\ e^{i(2\pi z n_1 {}^{v_0}/c - \omega t)}$$
$$+ \mathbf{Ev_2}\frac{\mathbf{E_0}\cdot\mathbf{Ev_2^*}}{\mathbf{Ev_2}\cdot\mathbf{Ev_2^*}}\ e^{i(2\pi z n_2 {}^{v_0}/c - \omega t)} \qquad (8)$$

After the resulting electric field $\mathbf{E_f}$ has been constructed, all that remains is a filter operation by applying a crossed polarizer. This filtering operation is performed by projecting the resulting field $\mathbf{E_f}$ onto the interrogation polarizer $\mathbf{P_I} = (P_x, P_y, 0)$. The values P_x and P_y are complex allowing for polarization interrogation for circular as well as linear polarization. Then the transmission can be determined by dividing the magnitude squared of the resulting electric field by the magnitude squared of the initial E field.

$$T(z,\theta) = \frac{(\mathbf{E_f}(z,\theta)\cdot\mathbf{P_I})(\mathbf{E_f}(z,\theta)\cdot\mathbf{P_I})^*}{\mathbf{E_0}\cdot\mathbf{E_0^*}} \qquad (9)$$

As an example, the Faraday case will be examined. For the Faraday Effect, $\theta = 0$ and we assume without loss of generality that the E field only has an E_x polarization and that the interrogation polarizer is oriented along the y-axis, then for the Faraday Effect case the roots from the determinant of the dispersion matrix and the Eigenvectors are:

$$n_1^2 = \frac{\epsilon_x - i\epsilon_{xy}}{\epsilon_0}, \qquad n_2^2 = \frac{\epsilon_x + i\epsilon_{xy}}{\epsilon_0} \qquad (10)$$

$$\mathbf{Ev_1} = \{i,1,0\}, \ \mathbf{E\,v_2} = \{-i,1,0\}. \qquad (11)$$

Using these to construct the transmission through the filter yields the Faraday Effect transmission T_f equation.

$$T_f(z) = \frac{1}{4}\left[e^{\frac{2i\pi z v_0\sqrt{\epsilon_x - i\epsilon_{xy}}}{c\sqrt{\epsilon_0}}} - e^{\frac{2i\pi z v_0\sqrt{\epsilon_x + i\epsilon_{xy}}}{c\sqrt{\epsilon_0}}} \right]$$
$$\times \left[e^{\frac{2i\pi z v_0\sqrt{\epsilon_x - i\epsilon_{xy}}}{c\sqrt{\epsilon_0}}} - e^{\frac{2i2i\pi z v_0\sqrt{\epsilon_x + i\epsilon_{xy}}}{c\sqrt{\epsilon_0}}} \right]^* \qquad (12)$$

For the Voigt Effect case $\theta = \pi/2$ and we assume the polarization of the E field Ex = Ey, and the interrogation polarizer is rotated 90 degrees relative to the incident electric field polarization. The roots and the associated Eigenvectors are given:

$$n_1^2 = \frac{1}{\epsilon_0}\left(\epsilon_x + \frac{\epsilon_{xy}^2}{\epsilon_x}\right), \qquad n_2^2 = \frac{\epsilon_z}{\epsilon_0} \qquad (13)$$

$$\mathbf{Ev_1} = \left\{0, \frac{\epsilon_x}{\epsilon_{xy}}, 1\right\}, \ \mathbf{E\,v_2} = \{1,0,0\}. \qquad (14)$$

The resulting transmission T_v for the Voigt configuration is

$$T_v(z) = \frac{1}{4}\left[\frac{\epsilon_x\epsilon_x^* \, e^{\frac{2i\pi z v_0\sqrt{\frac{\epsilon_{xy}^2}{\epsilon_x}+\epsilon_x}}{\sqrt{\epsilon_0}c}}}{|\epsilon_x|^2 + |\epsilon_{xy}|^2} + e^{\frac{2i\pi z v_0\sqrt{\epsilon_z}}{c\sqrt{\epsilon_0}}} \right]$$
$$\times \left[\frac{\epsilon_x\epsilon_x^* \, e^{\frac{2i\pi z v_0\sqrt{\frac{\epsilon_{xy}^2}{\epsilon_x}+\epsilon_x}}{\sqrt{\epsilon_0}c}}}{|\epsilon_x|^2 + |\epsilon_{xy}|^2} + e^{\frac{2i\pi z v_0\sqrt{\epsilon_z}}{c\sqrt{\epsilon_0}}} \right]^*. \qquad (15)$$

The general case for arbitrary θ can be solved analytically using a mathematical tool such as Mathematica. Unfortunately, while an analytic solution exists, it is approximately 200 pages of equations and therefore will not be printed here.

In order to evaluate the magneto-optical transmission the elements of the dielectric tensor ϵ_x, ϵ_{xy}, and

ϵ_z must be calculated. From Yariv [14], in general the dielectric tensor can be related to the polarizability tensor by $\epsilon_{ij} = \epsilon_0(1 + \chi_{ij})$. For the instance the magnetic field is aligned along the z-axis, the dielectric tenser is written in the gyrotropic form

$$\begin{bmatrix} \epsilon_x & \epsilon_{xy} & 0 \\ -\epsilon_{xy} & \epsilon_x & 0 \\ 0 & 0 & \epsilon_z \end{bmatrix}. \qquad (16)$$

This matrix can be diagonalized by calculating the Eigenvalues and relating the result to the polarizability tensor.

$$\begin{bmatrix} \epsilon_x - i\,\epsilon_{xy} & 0 & 0 \\ 0 & \epsilon_x - i\,\epsilon_{xy} & 0 \\ 0 & 0 & \epsilon_z \end{bmatrix} = \epsilon_0 + \epsilon_0 \begin{bmatrix} \chi_+ & 0 & 0 \\ 0 & \chi_- & 0 \\ 0 & 0 & \chi_z \end{bmatrix} \qquad (17)$$

Using this relationship allows the dielectric tensor elements to be related to the elements of the polarizability tensor χ

$$\epsilon_x = \frac{\epsilon_0}{2}(2 + \chi_+ + \chi_-), \quad \epsilon_{xy} = \frac{\epsilon_0}{2}i(\chi_- - \chi_+),$$
$$\epsilon_z = \epsilon_0(1 + \chi_0) \qquad (18)$$

where $\chi_\pm$ and χ_0 are the elements of the polarizability tensor for the $\sigma^\pm$ and π dipole allowed transitions respectively.

B. Polarizability Tensor

With the completion of a generalized method for propagating a plane wave through a dispersive medium, the next step is the characterization of the dispersive medium. The characterization of the medium is accomplished by calculating the polarizability tensor. Such a representation should take into account the atomic hyperfine splitting, Zeeman splitting, the motion of the atoms (Doppler Effect) the Boltzmann distribution of the energy level population and include the line strength for each dipole allowed transition. There are many examples in the literature which demonstrate the computation of the polarizability tensor χ. This work uses Dressler[2] as a model for computing the polarizability tensor.

Starting with an atom in the presence of an external magnetic field B₀, the total angular momentum F = I + J (where I is the nuclear spin and J is the orbital angular momentum) can be projected along the axis of the magnetic field yielding a good quantum number m. In the presence of a magnetic field the atomic hyperfine levels shift, split and cross. The result is the Zeeman split levels. The subsequent energy levels can be represented by the total Hamiltonian

$$H = H_{hfs} + H_z, \qquad (19)$$

which is the sum of the hyperfine split and the Zeeman split energy levels. The matrix elements for the Hamiltonian [15] are given by the following equation

$$\langle IJFm|H|IJF'm\rangle = \frac{1}{2}\delta_{F,F'}\left(AK + B\frac{(3K(K+1) - 2I(I+1)*2J(J+1))}{2I(2I-1)*2J(2J-1)} \right.$$
$$+ 2C\frac{5K^2\left(\frac{1}{4}K+1\right) + K\big(I(I+1) + J(J+1) + 3 - 3I(I+1)J(J+1)\big) - 5I(I+1)J(J+1)}{I(I-1)(2I-1)J(J-1)(2J-1)} \Bigg)$$
$$+ \frac{\mu_B g_J B_0}{h}(-1)^{(I+J+m+1)}\sqrt{J(J+1)\,(2J+1)\,(2F+1)\,(2F'+1)}\begin{Bmatrix} J & 1 & J \\ F' & I & F \end{Bmatrix}\begin{bmatrix} F & 1 & F' \\ -m & 0 & m \end{bmatrix}$$
$$- \frac{\mu_N g_I B_0}{h}(-1)^{(I+J+m+1)}\sqrt{I(I+1)\,(2I+1)\,(2F+1)\,(2F'+1)}\begin{Bmatrix} I & 1 & I \\ F' & J & F \end{Bmatrix}\begin{bmatrix} F & 1 & F' \\ -m & 0 & m \end{bmatrix} \qquad (20)$$

where K is given by

$$K = F(F+1) - J(J+1) - I(I+1) \qquad (21)$$

μ_B is the Bohr magneton, μ_N is the nuclear Bohr magneton, g_J is the Lande g factor, g_I is the nuclear g factor, A, B and C are the magnetic dipole, electric quadrupole and the magnetic octupole constants, respectively.

The energy levels for the atom in the external magnetic field are found by solving for the Eigenvalues and the normalized Eigenvectors of the Hamiltonian. The Eigenvalues represent the energy level shift $\Delta\nu_M$ relative to the center-of-gravity ν_0. The Eigenvector represents the mixing of the hyperfine split levels which result in the Zeeman split levels. The Eigenvalues are represented by the Magnetic quantum number M and the Eigenvectors by Y_M^{Fm}. The Zeeman spectrum arrives from the dipole allowed transitions $\Delta M = 0$ for π (linearly polarized) and $\Delta M = \pm1$ for $\sigma^\pm$ (circularly polarized). The Zeeman line strengths are given by

$$S_q(M, M') = \left|\langle IJM|d_q|IJ'M'\rangle\right|^2, \qquad (22)$$

wher M and M' represent the Eigenvalues or energy levels of the lower and upper levels respectively, d_q is the spherical component of the atomic dipole moment vector $\mathbf{d}$ and q = ΔM = $\pm1,0$. Recasting this expression in terms of the total angular momentum F and its projection m and explicitly maintaining the relationship to the magnetic quantum number M results in the following equation

$$S_q(M, M') = \left\{ \sum_{Fm}\sum_{F'm'} Y_M^{Fm}\langle IJFm|d_q|IJ'F'm'\rangle Y_{M'}^{F'm'} \right\}^2 \qquad (23)$$

where the un-primed and primed quantities represent the lower and upper states respectively. The matrix element $\langle IJFm|d_q|IJ'F'm'\rangle$ [16] is given by

$$\langle IJFm|d_q|IJ'F'm'\rangle = (-1)^{F-m}\begin{bmatrix} F & 1 & F' \\ -m & q & m' \end{bmatrix}$$
$$\times (-1)^{I+J'+F+1}\sqrt{(2F+1)(2F'+1)}$$
$$\times \sqrt{\frac{3c^3 h(2J'+1)\epsilon_0}{16\pi^3\nu_0^3\tau}}\begin{Bmatrix} J & I & F \\ F' & 1 & J' \end{Bmatrix}. \qquad (24)$$

The interaction with the atom for a resonant electromagnetic wave has now been characterized by the line strength $S_q(M, M')$. What remains is to obtain an expression for χ the polarizability tensor. The polarizability χ is defined as the ratio of the induced dipole moment to the applied electric field. The dipole moment can be written $\mathbf{D} = 1/2\,\chi\epsilon_0\mathbf{E}_0\exp[i(\mathbf{k}\cdot\mathbf{r} - \omega t)] + c.c.$ where ϵ_0 is the electric-permittivity constant. Similarly the induced dipole moment can be written for each of the Zeeman energy levels [17], assuming the wavelength of the applied electromagnetic wave is significantly longer than the atomic radius, as

$$\mathbf{D}_M = \frac{e^2}{2h}\sum_{M'} \frac{[\langle M|\mathbf{r}|M'\rangle \cdot \mathbf{E}_0]\langle M'|\mathbf{r}|M\rangle}{\nu_0 + \Delta\nu_{M,M'} - \nu - i/4\pi\tau} \times e^{i(\mathbf{k}\cdot\mathbf{r}-\omega t)} + c.c. \qquad (25)$$

3

where $\Delta\nu_{M,M'}$ are the frequency shifts due to the Zeeman splitting and τ is the natural lifetime of the ^{2}P state. A comparison of these two representations for the dipole moment will yield a representation for the polarizability tensor elements to be given by

$$\chi_M^q = \frac{e^2}{\epsilon_0 h}\sum_{M'}\frac{|\langle M|r_q|M'\rangle|^2}{\nu_0 + \Delta\nu_{M,M'} - \nu - i/4\pi\tau}. \qquad (26)$$

Making the equivalent substitution $e^2|\langle M|r_q|M'\rangle|^2 = |\langle M|d_q|M'\rangle|^2 = S_q(M,M')$ allows the polarizability tensor to be recast in terms of the line strengths of each dipole allowed transition.

$$\chi_M^q = \frac{1}{\epsilon_0 h}\sum_{M'}\frac{S_q(M,M')}{\nu_0 + \Delta\nu_{M,M'} - \nu - i/4\pi\tau} \qquad (27)$$

The polarizability tensor is a result of the interaction of a resonant electromagnetic plane wave propagating through a volume of atoms represented by the number density N_M for each lower state $|M\rangle$. Since each of these particles is moving at a different velocity u the center-of-gravity frequency ν_0 must be replaced by a Doppler shifted frequency $\nu_0(1 + u/c)$. Then, integrating over the Maxwellian velocity distribution to account for all velocity groups

$$f(u)du = N_M\sqrt{\frac{M_0}{2\pi kT}}e^{\frac{-M_0 u^2}{kT}}du \qquad (28)$$

where M_0 is the mass of the atom, T is the temperature of the cell and k is Boltzmann's constant. Finally, the Doppler corrected polarizability tensor can be expressed as

$$\chi_M^q = \frac{1}{\epsilon_0 h}\times\int_{-c}^{c}\left(\sum_{M'}\left[\frac{S_q(M,M')}{\nu_0(1+\frac{u}{c}) + \Delta\nu_{M,M'} - \nu - \frac{i}{4\pi\tau}}\right]\right)$$
$$\times\left(N_M\sqrt{\frac{M_0}{2\pi kT}}e^{\frac{-M_0 u^2}{kT}}\right)du. \qquad (29)$$

Since each state $|M\rangle$ represents a different energy level then the population of each of these levels must conform to a Boltzmann distribution. Therefore, each number density $N_M = N_0 B_M$ where N_0 is the total number density and B_M is the Boltzmann distribution for the $|M\rangle$ level given by

$$B_M = \frac{e^{\frac{-h\Delta\nu_M}{kT}}}{\sum_M e^{\frac{-h\Delta\nu_M}{kT}}}. \qquad (30)$$

The total bulk polarizability tensor is found by summing equation (29) over the lower states $|M\rangle$. Utilizing the plasma dispersion function

$$W(z) = \frac{i}{\pi}\int_{-\infty}^{\infty}\frac{e^{-t^2}}{z-t}dt = e^{-z^2}\text{Erfc}[z/i] \qquad (31)$$

which is related to the complementary error function (Erfc). The total polarizability tensor can be written as

$$\chi_q(\nu) = \frac{iN_0}{\epsilon_0 h\nu_0}\sqrt{\frac{\pi M_0 c^2}{2kT}}\sum_{MM'}[B_M S_q(M,M')W(\xi)]$$
$$\xi = \sqrt{\frac{\pi M_0 c^2}{2kT}}\left(\frac{\nu_0 - \nu - \Delta\nu_{M,M'}}{\nu_0} + \frac{i}{4\pi\nu_0\tau}\right) \qquad (32)$$

Using equations 30, 31, and 32 χ_+, χ_-, and χ_0 can be calculated for each frequency ν and substituted back into equations 7, 8, and 9 to arrive at the predicted transmission through the GMOT filter.

3. EXPERIMENTAL APPARATUS

The best way to validate the outlined model is to compare the model's predictions to laboratory measurements. To that end, an experiment using the configuration illustrated in fig. 1 was conducted.
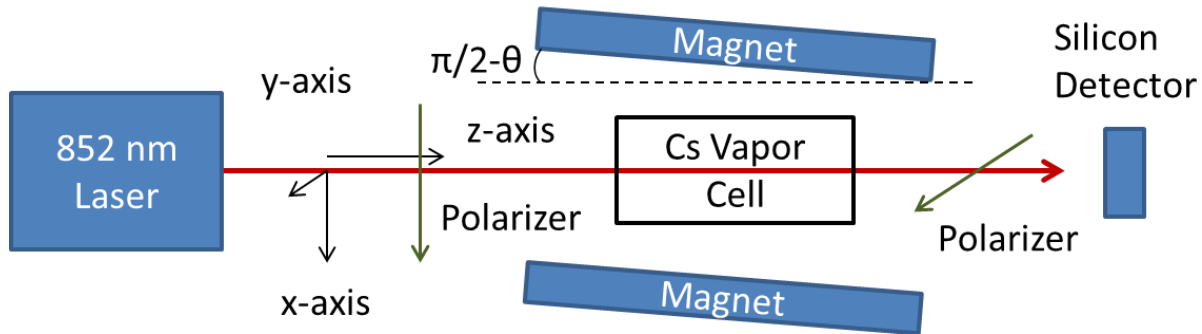

Fig. 1. Magneto-optical filter experimental apparatus.

The experiment consisted of a tunable 852 nm laser (500 KHz line width and a mode-hop-free tuning range of 15 – 30 GHz) propagated through crossed polarizers with a heated cesium vapor cell situated between the polarizers. Additionally, a magnetic field was applied to the vapor cell. The magnetic field could be oriented at $\theta = 0$, 90 degrees and values in between. Finally, the laser beam was detected by a silicon detector and the resulting spectrum was recorded with an oscilloscope.

Three separate experiments were conducted to validate the model. The first case was the standard Faraday configuration, $\theta = 0$, with an applied magnetic field of 300 Gauss, a cell temperature of 58 C, a cell length of 7.5 cm and the laser beam initially polarized along the x-axis and interrogated by a polarizer aligned along the y-axis. Figures 2 and 3 show the experimental and the theoretical spectra. The experiment and calculated results are in good agreement considering the uncertainty in the absolute temperature, the homogeneity of the magnetic field and fluxuations in laser power.
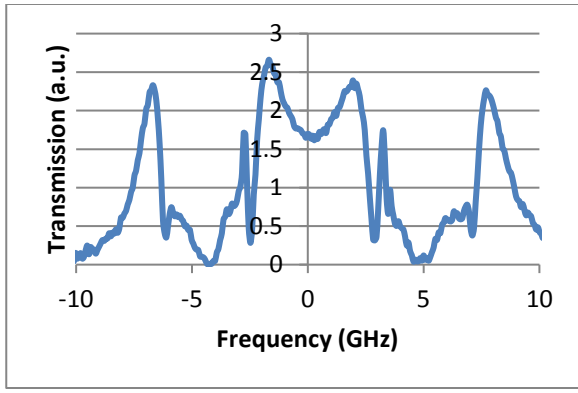
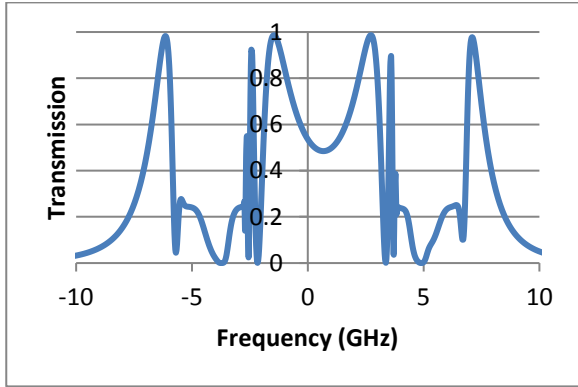Fig. 2. Experimental Faraday transmission with B = 300 Gauss, T = 58 C, L=7.5 cm, and θ = 0 degrees.

Fig. 3. Theoretical Faraday transmission with B = 300 Gauss, T = 58 C, L=7.5 cm, and θ = 0 degrees.

The second case was the standard Voigt configuration, θ = 90 degrees, with an applied magnetic field of 700 Gauss, a cell temperature of 84 C, a cell length of 7.5 cm and the laser beam initially polarized at 45 degrees relative to the x-axis and interrogated by a polarizer aligned to -45 degrees relative to the x-axis. Figures 4 and 5 show the experimental and the theoretical spectra. The experiment and calculated results are in good agreement considering the normal experimental uncertainty in the absolute temperature, the homogeneity of the magnetic field and probe laser power fluxuations.
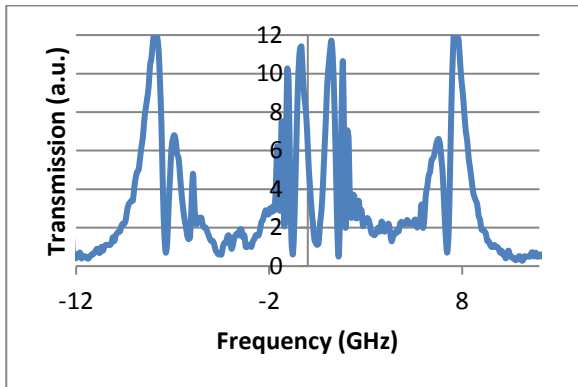

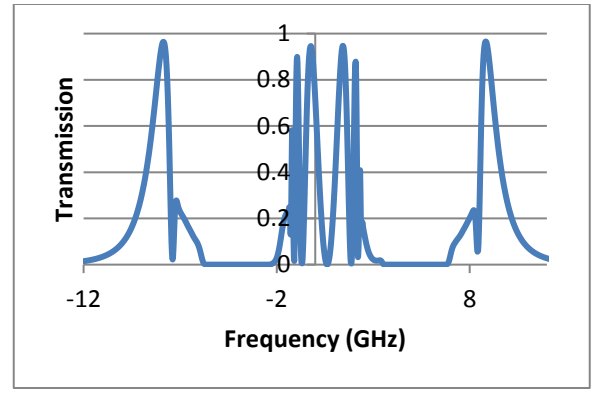Fig. 4. Experimental Voigt transmission with B = 700 Gauss, T = 84 C, L = 7.5 cm, θ = 90 degrees.

Fig. 5. Theoretical Voigt transmission with B = 700 Gauss, T = 84 C, L = 7.5 cm, θ = 90 degrees.

For the last case the angle between the magnetic field and the probe laser was set to θ = 87 degrees, with an applied magnetic field of 500 Gauss, a cell temperature of 100 C, a cell length of 7.5 cm and the laser beam initially polarized along the x-axis and interrogated by a polarizer aligned along the y-axis. Figures 6 and 7 show the experimental and the theoretical spectra. The experiment and calculated results are in good agreement considering the uncertainty in the absolute temperature, the homogeneity of the magnetic field and fluxuations in laser power.
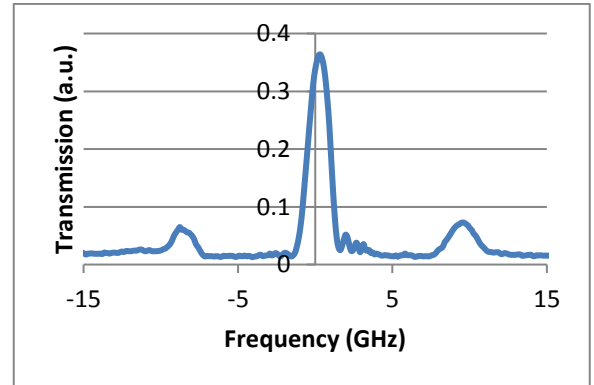

Fig 6. Experimental GMOT with B = 500 Gauss, T = 100 C, L = 7.5 cm, θ = 87 degrees.
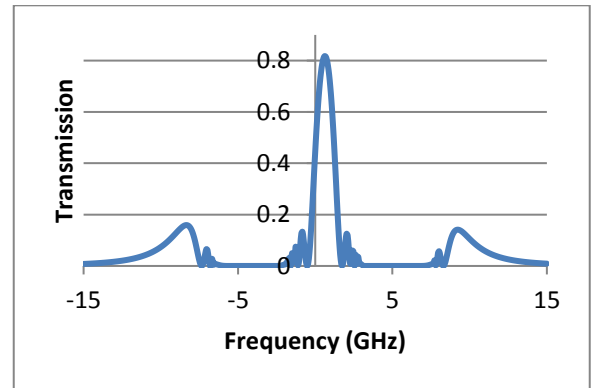

Fig 7. Theoretical GMOT with B = 500 Gauss, T = 100 C, L = 7.5 cm, θ = 87 degrees.

An examination of the three test cases in figures 2-7 used to verify the efficacy of the model demonstrates good

agreement between the experimental and theoretical spectra. This is true even over a wide range of magnetic field and temperature variations. Given the good agreement between theory and experiment, it is now possible to use the model to perform filter optimization.

4. OPTIMIZED FILTER

To demonstrate the usefulness of a GMOT solution for magneto-optical scattering we will compare an optimized Faraday filter to a GMOT filter. To do this we have drawn from the work of Zentile [18]. Zentile presents an idealized case for a cesium filter. The quality of the filter is quantified by the use of two metrics. The first metric is the equivalent noise bandwidth (ENBW):

$$\text{ENBW} = \frac{\int_0^\infty T(\nu)d\nu}{T(\nu_s)}, \tag{33}$$

where T is the transmission through the filter and ν_s is the frequency at maximum transmission through the filter. The second metric is a figure of merit (FOM):

$$\text{FOM} = \frac{T(\nu_s)}{\text{ENBW}} \tag{34}$$

Using these metrics the general model was run for several cases to identify an optimized solution. The spectrum for such an optimized case is shown in figure 8, the recalculated case from the article is shown in figure 9, and a comparison of the metrics is provided in table 1.
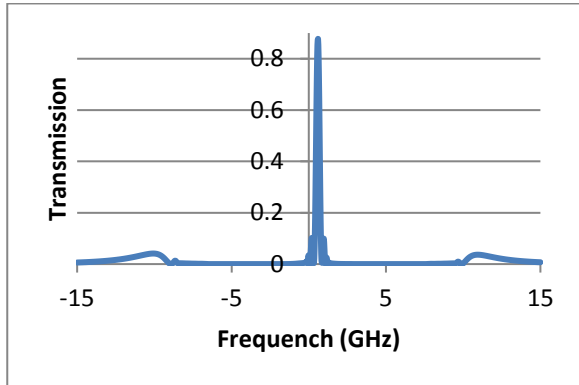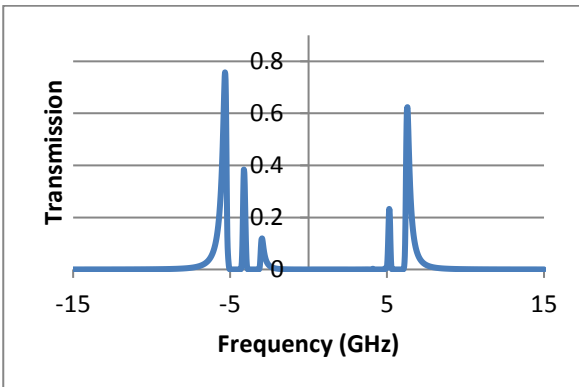

Fig. 8. A GMOT optimized filter.

Fig 9. A Faraday optimized filter.

Table 1. Referenced Faraday filter metrics compared to calculated Faraday filter and GMOT filter.

	Faraday [18]	Faraday calculated	GMOT
B (Gauss)	45.3	45.3	1000
T (C)	60	60	93
ENBW (GHz)	0.96	0.95	0.56
Max Transmission %	77	76	88
FOM (GHz^{-1})	0.80	0.80	1.56
FWHM (MHz)	310	308	250
Angle θ (degrees)	0	0	88
Transition	$S_{1/2} \rightarrow P_{1/2}$	$S_{1/2} \rightarrow P_{1/2}$	$S_{1/2} \rightarrow P_{3/2}$

A comparison of these two cases reveals that using a more generalized approach to magneto-optical filters can yield filters almost two times better than a standard Faraday configuration. From these results it is clear that a more generalized approach for examining magneto-optical scattering can yield significant benefits for light filtering and has significant potential for other applications.

5. CONCLUSION

This work has completed a model for the analysis of magneto-optical filters. The model includes all relevant elements for the accurate characterization of atomic media. These elements include the atomic hyperfine and Zeeman splitting of the energy levels, the Doppler Effect the Boltzmann distribution of the energy level population and line strength for each dipole allowed transmission. Additionally, the model accurately propagates a plane wave through a dispersive medium yielding a result that can predict the resulting spectrum for any relative angle between a plane wave direction of propagation and the applied magnetic field. This model was experimentally validated for both limiting cases Faraday and Voight in addition to a case with arbitrary angle of incidence. All three cases show good agreement between the theoretical predictions and the experimental spectra. In addition, the significance of examining magneto-optical filters for arbitrary angle cases was demonstrated by revealing an optimized filter with an equivalent noise bandwidth of 0.56 GHz which is approximately a factor of two better than those previously reported.

References

1. E. D. Palik and J. K. Furdyna, "Infrared and microwave magnetoplasma effects in semiconductors", Rep. Prog. Phys., 33, 1193-1322 ,(1970).
2. E. Dressler, A. Laux, and R. Billmers, "Theory and experiment for the anomalous Faraday effect in potassium", J. Opt. Soc. Am. B, Vol. 13, No. 9, (1996).
3. P. S. Pershan, "Magneto-Optical Effects", J. Appl. Phys., 38, (1967).
4. J. Halpern, B. Lax, and Y. Nishina, "Quantum Theory of Interband Faraday and Voigt Effects", Phys. Rev., Vol. 134, No. 1A, (1964).
5. Cord Fricke-Begemann, Matthias Alpers, and Josef Höffner , "Daylight rejection with a new receiver for potassium resonance temperature lidars", Optics Letters, Vol. 27, Issue 21, pp. 1932-1934, (2002).
6. H. Chen, M. A. White, David A. Krueger, and C. Y. She , "Daytime mesopause temperature measurements with a sodium-vapor dispersive

Faraday filter in a lidar receiver", Optics Letters, Vol. 21, Issue 15, pp. 1093-1095, (1996).

7. Wentao Huang, Xinzhao Chu, B. P. Williams, S. D. Harrell, Johannes Wiig, and C.-Y. She , "Na double-edge magneto-optic filter for Na lidar profiling of wind and temperature in the lower atmosphere", Optics Letters, Vol. 34, Issue 2, pp. 199-201, (2009).

8. Tang Junxiong, Wang Qingji, Li Yimin, Zhang Liang, Gan Jianhua, Duan Minghao, Kong Jiankun, and Zheng Lemin , "Experimental study of a model digital space optical communication system with new quantum devices", Applied Optics, Vol. 34, Issue 15, pp. 2619-2622, (1995).

9. Joanna A. Zielińska, Federica A. Beduini, Vito Giovanni Lucivero, and Morgan W. Mitchell, "Atomic filtering for hybrid continuous-variable/discrete-variable quantum optics", Optics Express, Vol. 22, Issue 21, pp. 25307-25317, (2014).

10. T. Sakurai, K. Tanaka, H. Miyazaki, K. Ichimoto, A. Sakata, and S. Wada, "Construction of long-life magneto-optical filters for helioseismology observations", Progress of Seismology of the Sun and Stars, Lecture Notes in Physics, Vol., 367, pp., 277-280, (1990).

11. Manabu Yamamoto and Seiichi Murayama, "Analysis of resonant Voigt effect", J. Opt. Soc. Am., Vol. 69, No. 5, (1979).

12. J. Menders, P. Searcy, K. Roff, and Eric Korevaar , "Blue cesium Faraday and Voigt magneto-optic atomic line filters", Optics Letters, Vol. 17, No. 19, (1992).

13. J. Kankar and R. Stephens, "Signal-t~noise ratio characteristics of the atomic Voigt effect", Spectrochimica Acta, Vol. 38B, No. 10, (1983).

14. A. Yariv and P. Yea, "Optical Waves in Crystals", Wiley-Interscience, p. 70, (2003).

15. D. A. Steck, "Cesium D Line Data" Oregon Center for Optics and Department of Physics, University of Oregon, (1998).

16. Igor I. Sobelman, "Atomic Spectra and Radiative Transitions", Springer-Verlag, 2nd Edition, pp.,70-90, (1992).

17. P. Yeh, ''Dispersive magnetooptic filters,'' Appl. Opt. 21, 2069–2075 (1982).

18. M. Zentile, D. Whiting, J. Keaveney, C. Adams, and I. Hughes "Atomic Faraday filter with equivalent noise bandwidth less than 1 GHz", Optics Letters, Vol. 40, No. 9, (2015).